

DEVELOPMENT AND PERFORMANCE CHARACTERISTICS OF A NEW pH ELECTRODE

J. G. Connery, R.D. Baxter and C. W. Gulczynski
Leeds & Northrup
A Unit of General Signal
North Wales, Pennsylvania 19454

Presented at the
1992 Pittsburgh Conference

New Orleans, LA
March 10, 1992
Paper #561

In the late 1960's, the Dutch researcher, Piet Bergveld, investigated the pH sensitivity of an electronic device known as an ion-sensitive or ion-selective field-effect transistor (ISFET). Although early ISFETs undoubtedly responded to pH, many had considerable performance problems, including poor stability, slow response time to changes in pH and sub-Nernstian output. In the twenty plus years since Bergveld's initial efforts, ISFET technology has been substantially advanced primarily through the efforts of groups located in Holland, Japan, and the United States.

Leeds & Northrup's Solid State Physics and Chemistry Research groups began to look at ISFET sensor technology in the 1980's because of the Company's long-standing interest in pH measurement. Many problems were found in early ISFET devices. In the process of understanding and correcting the deficiencies of these devices, L&N has substantially advanced ISFET technology. This is represented in four L&N patents to date, and proprietary

semiconductor materials and processing techniques. Nine ISFET electrodes, under the tradename of DURAFET™, have been developed together with four electronics adaptors which interface DURAFET electrodes to existing commercial instrumentation.

The following describes the development and performance characteristics of ISFET-based DURAFET pH electrodes.

Development

The ISFET sensor begins as a silicon wafer. The silicon wafer is either n (negative) or p (positive) doped. The n type wafer material is favored and is used to produce a p channel enhancement mode field-effect transistor. A p channel wafer is the preferred starting material because L&N has developed and patented a back-side electrical contact method which permits electrical contact to the back-side of the chip. The advantage of back-side contacting is the total isolation of the test sample from the attachment leads. A completed wafer is illustrated in Figure 1.

ISFET sensors are three terminal devices (Figure 2). The n type wafer material is one of the three terminals and is designated as the "n Silicon Substrate" in Figure 2. Two additional regions are boron diffused to produce p+ doped sites. At this stage in the fabrication process, the sensor is completely symmetrical.

In Figure 2, the designations of "source" and "drain" are associated with the voltages later applied to the p+ doped regions. By convention, the "source" lead, shown connected to the substrate, is the electrical reference point against which all voltages and currents are referred. Lastly, an insulator is deposited or formed on top of the structure. It responds to pH in a manner analogous to glass electrodes. For example, if solution pH increases by one pH unit, the potential at the insulator/solution interface becomes more negative by approximately

60 mV at room temperature. This 60 mV change is referenced to the source through the reference electrode and an external low impedance bias voltage V_{rs} .

Theory

For a p channel ISFET the increased negative insulator potential increases the conductance between the FET's drain and source terminals. A way this field effect can be verified is to apply an external drain to source bias, V_{ds} , and measure the resulting current, I_{ds} , which is related to FET conductance. It is possible to operate the FET in such a way that the measured current, I_{ds} , is directly proportional to pH. This is referred to as an amperometric-like mode of operation.

An alternative mode of operation requires maintaining the ISFET at constant I_{ds} and V_{ds} values in such a way that FET conductance is constant. Because it is operating at constant conductance, when the insulator becomes more negative by 60 mV, the external low impedance voltage V_{rs} must be adjusted by +60 mV to maintain constant FET conductance I_{ds} . This is referred to as a potentiometric mode of operation. In this mode of operation, changes in the V_{rs} mirror the changes in the potential developed at the insulator/solution interface.

Figure 3 illustrates the typical current voltage curves for DURAFET in a pH 4 buffer. The relationship between the three electrical parameters I_{ds} , V_{ds} and V_{rs} can be seen. They are negative in value as typi-

Continued

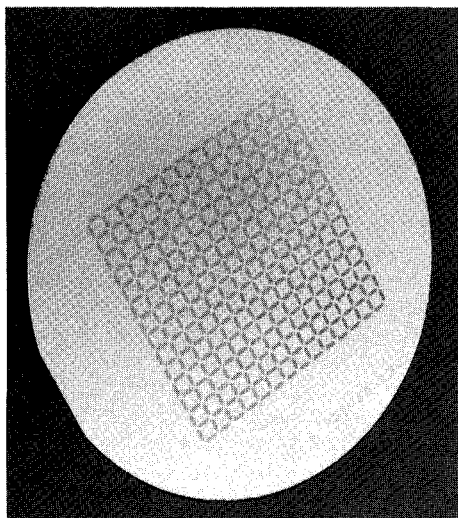
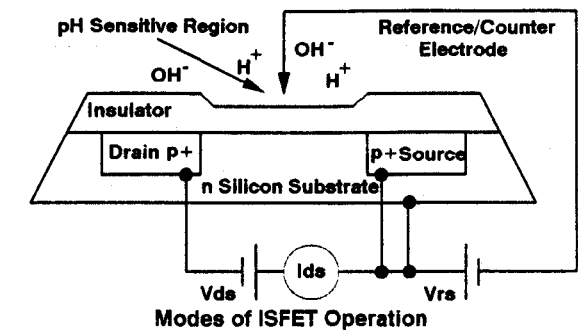


Figure 1 - View of an ISFET Wafer



LEEDS & NORTHROP
A UNIT OF GENERAL SIGNAL

Instrument & System Solutions!



Modes of ISFET Operation

Method	Operating Region	Control	Measure
Potentiometric	Linear or Saturation	V_{ds}, I_{ds}	V_{rs}
Amperometric	Linear Only	V_{rs}, V_{ds}	I_{ds}

Figure 2

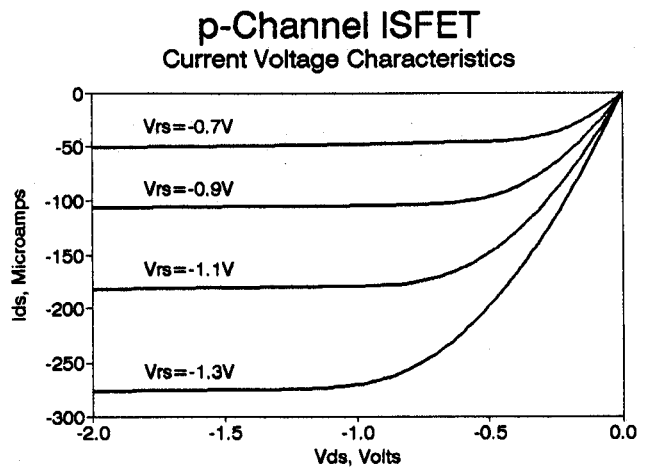


Figure 3

cally found for a p channel enhancement mode device. Amperometric type measurements are achieved in the linear region, at small V_{ds} values, where I_{ds} is linear with V_{ds} , V_{rs} and pH. At larger drain to source values, I_{ds} is independent of V_{ds} . This region is known as the saturation region and, because I_{ds} is proportional to the square root of V_{rs} and pH, amperometry is of little analytical utility.

While the amperometric type of pH measurement is largely limited to the linear region, the potentiometric mode allows for operation anywhere within the current-voltage curves. The potentiometric mode of operation is preferred in the saturation region because excellent Nernstian behavior is found, the measured EMF is independent of V_{ds} and performance is found to be independent of ISFET design geometries.

Experimental

Figure 4 illustrates typical measured V_{rs} values versus temperature against a 2N Ag/AgCl reference electrode. The data was collected on a typical ISFET device in 3 National Institute of Standards & Technology (NIST) standard reference buffers over a period of six days. Compared to glass electrode behavior, the voltage magnitude and temperature sensitivity appear to be most unusual.

A simple and accurate relationship between V_{rs} and pH and temperature has been determined. Equation (1) in Figure 5 contains the conventional pH term as if found with an ordinary glass electrode. In addition, a pH and temperature independent offset voltage designated as V_{rs}^0 and a pH independent temperature coefficient, designated as α , is illustrated. Simple differentiation of this equation with respect to temperature and, setting the result to zero, allows one to determine the pH value for zero dependence of voltage with temperature, referred to as isopotential pH. Furthermore, substitution of the resulting pH value into the parent relationship yields a V_{rs}^0 value

signal to V_{rs}^0 . V_{rs}^0 can be thought of as the electrode voltage at zero degrees Kelvin, the isopotential reference to source voltage, or the zero Kelvin standard potential of the ISFET. This equation predicts that a plot of $V_{rs}^0 - R(1n10)/F \times \text{pH} \times \text{Temperature}$ vs. Temperature should be a straight line whose zero Kelvin intercept defines the V_{rs}^0 value and whose slope is related to the electrode's isopotential pH value through equation (3) in Figure 5.

Figure 6 is a plot of this relationship, in a 4.006 buffer, vs. Celsius temperature, solely for the purposes of demonstrating linearity. Figure 7 is a plot of the same data where absolute temperature is used on both the x and y axes. As illustrated, V_{rs}^0 is observed to be a large magnitude voltage and an excellent one sigma value is obtained. From this analysis Nernstian behavior cannot be assumed a priori.

To test the Nernstian assumption, data obtained in NIST pH 4, 7 and 9 buffers is plotted in Figure 8. Excellent agreement between the zero Kelvin voltage and the pH 4 data is found. With knowledge of the zero Kelvin voltage and the temperature coefficient, or isopotential pH and isopotential voltage, it is possible to temperature compensate V_{rs} measurements fully.

Device-to-device values of V_{rs}^0 can vary over a range of plus or minus several hundred millivolts. While this variability is totally consistent with standard semiconductor manufacturing processes, means must be provided to correct for probe isopotential voltage. This semiconductor behavior has been accounted for by determining the V_{rs}^0 value of every single probe produced and by providing a hardware identification of the V_{rs}^0 value within each probe so that the electronics can correct each probe for its own unique V_{rs}^0 value. This approach allows for probe interchangeability.

The best fit of experimental data to temperature and pH, given the best pH values available, is illustrated in Figure 9. NIST pH data was employed between 0 and 50

degrees, and Bates' data, on highly purified buffer reagents, for temperatures between 60 and 90° C. The markers on the plot show the experimental data; the solid curves designate the NIST and Bates' data defining the conventionally true values. Excellent agreement between the experimental and conventionally true values is shown.

This relatively large amount of data obtained was subjected to multiple linear regression analysis to obtain isopotential (pH, EMF) values. At the same time, the evaluation of the Nernst slope, expressed as percent theoretical slope (PTS), was calculated at 99.4%. While specifications define PTS to be >96%, values are typically found between 99 and 100%. This illustration demonstrates the accuracy that can be obtained using DURAFET electrodes. In addition to accuracy, DURAFET electrodes exhibit excellent speed of response to pH changes.

Over 1000 individual measurements, collected at a rate of approximately 5 readings per second, on a typical DURAFET electrode, alternately immersed in NIST 4.01 and 6.86 buffers, are illustrated in Figure 10. The Y-axis of this plot is the voltage output of the adaptor electronics, which simulates the EMF output of a glass electrode at 25° C. When the adaptor electronics is connected to a suitable pH meter, excellent speed of response is observed and plotted in Figure 11.

Figure 12 is a semi-log plot of electronics EMF output which further demonstrates details of the pH response and output stability following the pH transition. The data shown in this figure was collected at a rate of 15 measurements/second for the first 25 seconds, followed by individual measurements at 2 minute intervals. A total of 1129 measurements over a 100,000 second period are illustrated. The pH transition begins at 5 seconds; for all practical purposes the final value is reached at 6 seconds. Figure 13 is the comparable

ISFET $V_{rs} = f(\text{pH}, \text{Temperature})$ in NIST Buffer Solutions

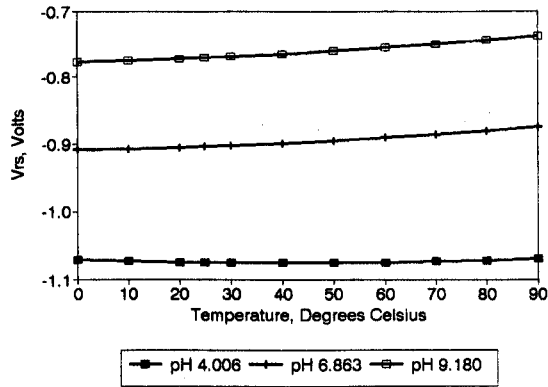


Figure 4

$$V_{rs} = V_{rs}^{\circ} + \frac{R (\ln 10)}{F} \text{pH}T + \alpha T \quad (1)$$

where : V_{rs}° = Iso-potential reference to source voltage

$$\frac{R (\ln 10)}{F} = \text{Nernst Factor}$$

T = Absolute Temperature

α = Electrode Temperature Coefficient

$$\frac{\partial V_{rs}}{\partial T} = \frac{R (\ln 10)}{F} \text{pH} + \alpha = 0 \quad (2)$$

$$\text{pH}_{iso} = \frac{-\alpha F}{R (\ln 10)} \quad (3)$$

Figure 5

Iso-potential V_{rs} Plot

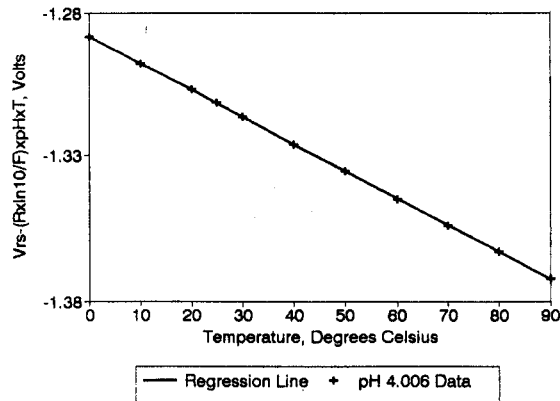


Figure 6

Iso-potential V_{rs} Plot

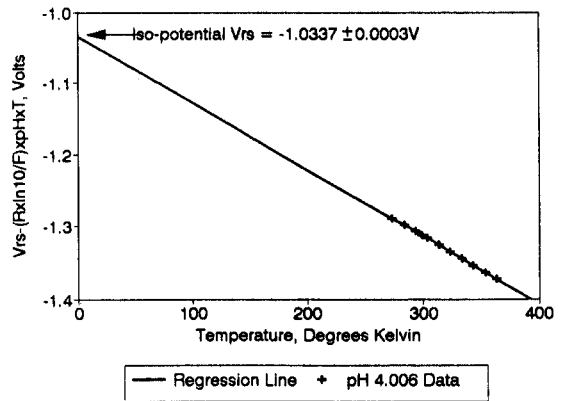


Figure 7

Iso-potential V_{rs} Plot

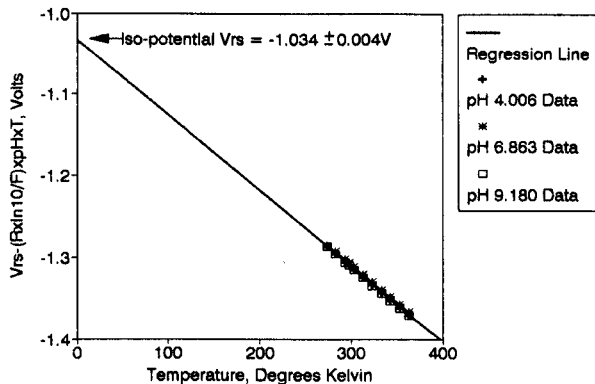


Figure 8

ISFET Temperature Performance in NIST Buffer Solutions

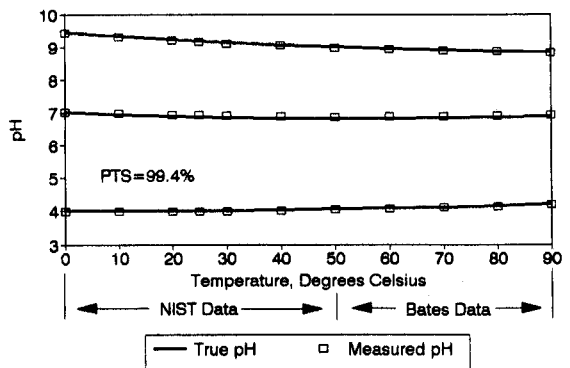


Figure 9

illustration when results are expressed in Engineering Units of pH. The one sigma value of the data in the 20-100,000 second interval is 0.002 pH.

Summary

Leeds & Northrup has developed a total of nine electrodes as well as interface electronics which compensate for the ISFET's

V_{rs}° value and for automatic Nernstian temperature compensation. The electronics output is intended to replicate the output of a glass electrode at 25° C and was designed to be compatible with commercial pH instrumentation.

DURAFET pH electrodes are of rugged design with back side contact for reliability. Excellent pH accuracy, over a wide tem-

perature range, fast speed of response and excellent long term stability have been demonstrated.

Acknowledgment

The authors acknowledge the many important contributions of the L&N Solid State Technology and Analytical Engineering staffs.

DURAFET™ Response Time
Between NIST type 4.01 and 6.86 Buffers

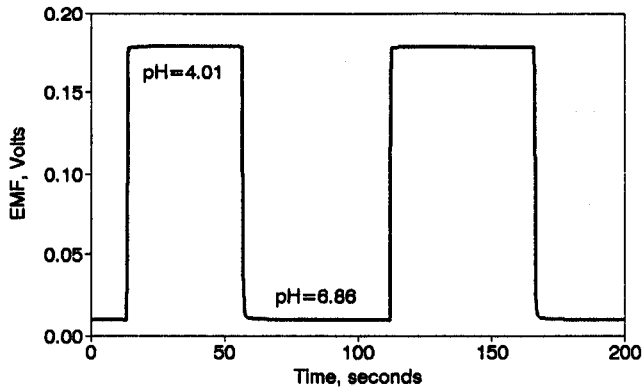


Figure 10

DURAFET™ Response Time
Between NIST type 4.01 and 6.86 Buffers

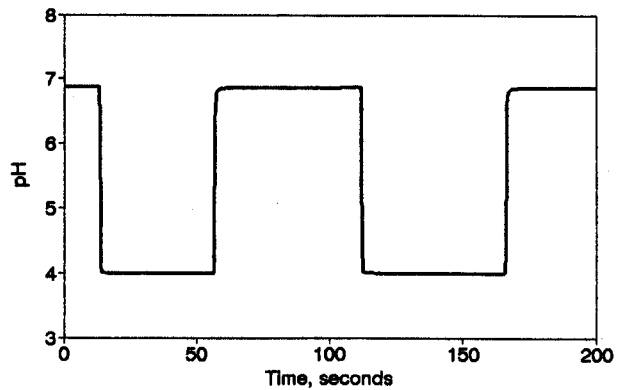


Figure 11

DURAFET™ Stability
in NIST 4.006 Buffer

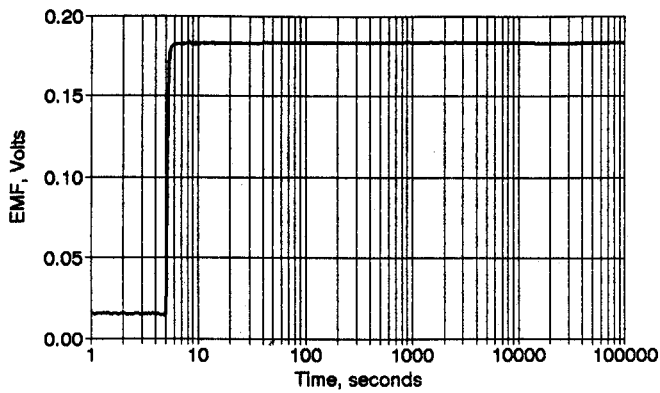


Figure 12

DURAFET™ Stability
in NIST 4.006 Buffer

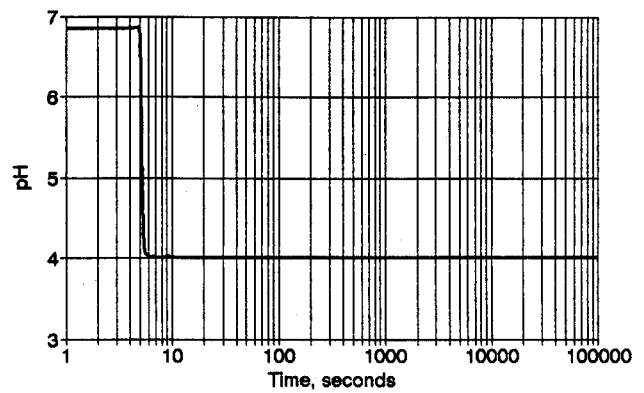


Figure 13



LEEDS & NORTHRUP
A UNIT OF GENERAL SIGNAL

Instrument & System Solutions!

351 Sumneytown Pike • P.O. Box 2000 • North Wales, PA 19454, USA • (215) 699-2000 • FAX (215) 699-3702